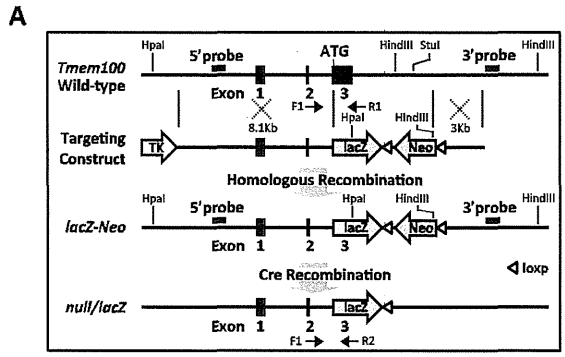

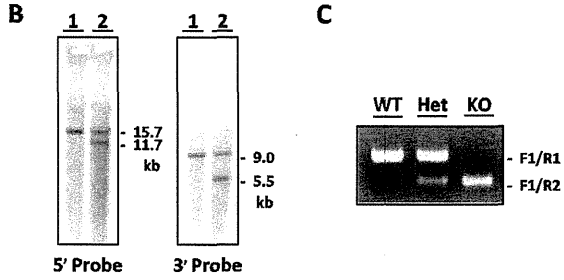

D

Stage	Total numbers	WT	Het	KO
E8.0	31	8 (25.8 %)	15 (48.4 %)	8 (25.8 %)
E8.5	29	7 (24.1 %)	16 (55.2 %)	6 (20.7 %)
E9.0	80	18 (22.5 %)	40 (50.0 %)	22 (27.5 %)
E9.5	304	78 (25.7 %)	152 (50.0 %)	74 (24.3 %)
E10.0	115	29 (25.2 %)	60 (52.2 %)	26 (22.6 %)
E10.5	94	29 (30.9 %)	55 (58.5 %)	10 (10.6 %)
E11.0	26	9 (34.6 %)	17 (65.4 %)	0 (0.0 %)
E12.5	21	7 (33.3 %)	14 (66.7 %)	0 (0.0 %)
E14.5	26	8 (30.8 %)	18 (69.2 %)	0 (0.0 %)
E16.5	16	6 (37.5 %)	10 (62.5 %)	0 (0.0 %)
P30	808	271 (33.5 %)	537 (66.5 %)	0 (0.0 %)

Fig. S3. Genotyping and survival of *Tmem100* null mice. (*A*) Schematic diagram represents the *Tmem100* targeting strategy. (*B*) Southern blot analysis of control (lane 1) and *Tmem100* targeted (lane 2) ES cells. (*C*) A representative result of PCR genotyping using yolk sac. Het, heterozygous; KO, homozygous null; WT, wild type. Positions of the 5′ and 3′ probes for Southern blot analysis and PCR genotyping primers (F1, R1, and R2) are shown in *A*. (*D*) Frequency of genotypes obtained from *Tmem100* Het–Het mating on a C57BL/6 genetic background. *Tmem100* null embryos die in utero by E11.0. E, embryonic day; P, postnatal day.

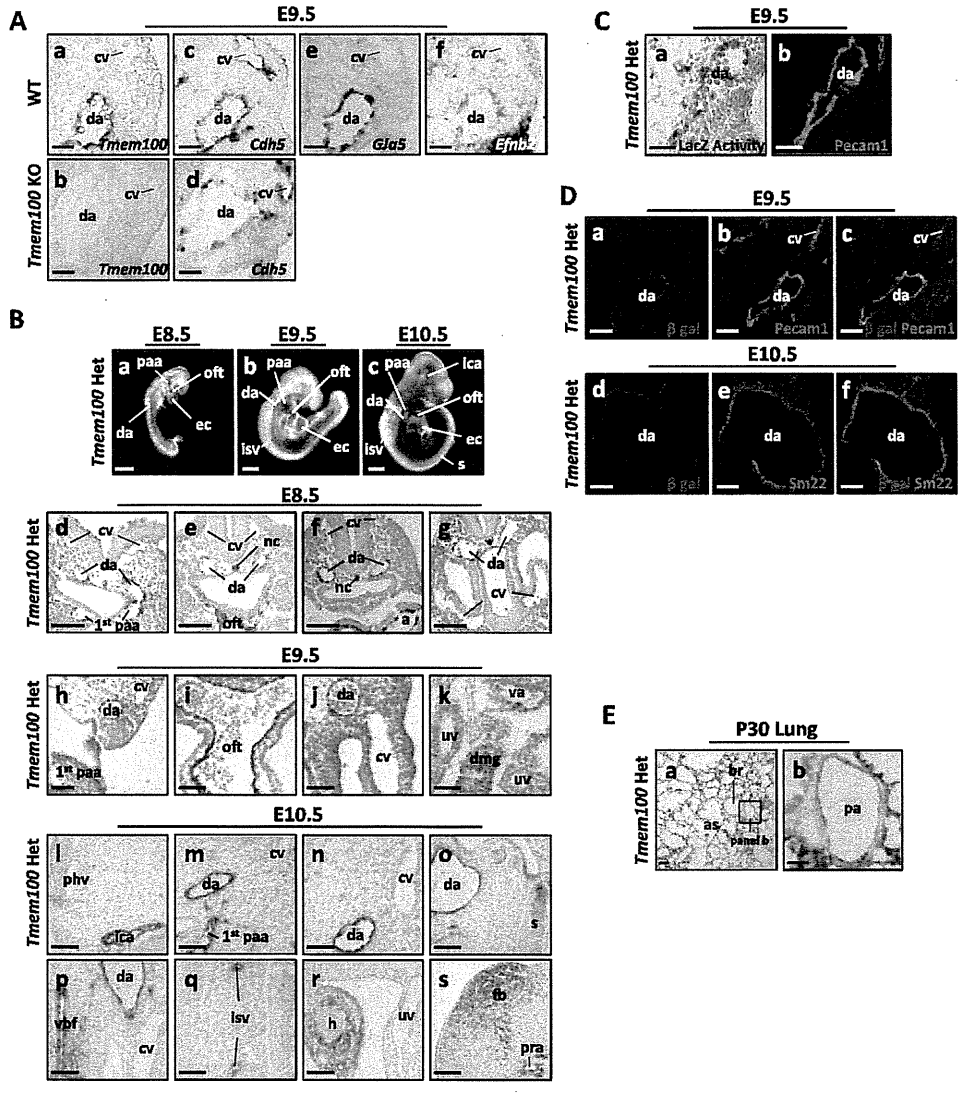

Fig. S4. Arterial endothelium-enriched expression of *Tmem100* during vascular development in mouse embryos. (*A*) Confirmation of arterial endothelium expression of *Tmem100* mRNA (a) by in situ hybridization using serial sections of mouse embryos. *Gja5/Cx40* (e) and *Efnb2* (f) are shown as arterial endothelium makers, and *Cdh5* (c) is shown as a nonspecific endothelium marker that is expressed in both arterial and venous endothelial cells. Absence of *Tmem100* signals in *Tmem100* null embryos (*b*), where *Cdh5* expression is kept intact (*d*), serves as a negative control. (*B*) Knock-in lacZ reporter activity is mainly detected in various arteries and endocardium, but not in veins, in *Tmem100* heterozygous embryos at E8.5–10.5. Whole-mount stains (*a–c*) and their sections (*d–s*) are shown. (*C*) LacZ reporter activity is detected in Pecam1-positive endothelial cells of dorsal aorta in *Tmem100* heterozygous embryos at E9.5. LacZ staining and immunohistochemistry of serial sections are shown. *b* is shown with nuclear DAPI stain. (*D*) LacZ-encoded β-galactosidase (β-gal) protein is colocalized with Pecam1, but not with Sm22, in dorsal aorta of *Tmem100* heterozygous embryos. Immunohistochemistry is shown. *b*, *c*, *e*, and *f* are shown with nuclear DAPI stain. (*E*) In the lung of *Tmem100* heterozygous mice at postnatal day 30 (P30), lacZ activity is detected in the endothelium of pulmonary vasculature and alveoli, but not in airway epithelial cells. as, alveolar space; br, bronchiole; cv, cardinal vein; da, dorsal aorta; dmg, dorsal mesentery of gut; fb, forelimb bud; h, hindgut; ica, internal carotid artery; isv, intersomitic vessel; nc, notochord; oft, outflow tract; pa, pulmonary artery; paa, pharyngeal arch artery; phv, primary head vein; pra, principal artery; s, somite; uv, umbilical vein; va, vitelline artery; vbf, ventral bifurcation of foregut to produce tracheal diverticulum. (Scale bars: *A*, *C*, and *D*, 20 μm; *B*, *a–c*, 200 μm; and *B*, *d–s*, and *E*, 50 μm.)

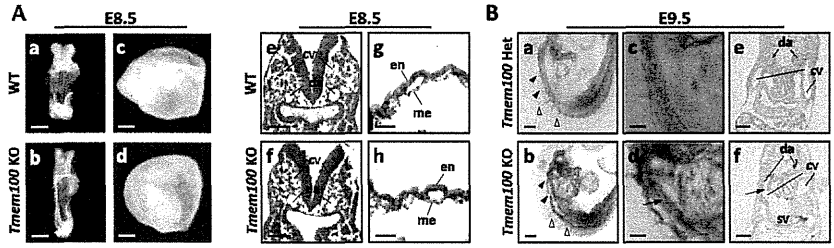

Fig. S5. *Tmem100* null embryos: absence of vascular phenotypes at E8.5 and arteriovenous malformation at E9.5. (*A*) *Tmem100* null embryos and yolk sac have no detectable abnormalities of vascular structure at E8.5. Gross appearance (*a–d*) and H&E-stained sections (*e–h*) are shown. (*B*) At E9.5, *Tmem100* null embryos have aberrant arteriovenous connections between dorsal aorta and cardinal vein, as marked with arrows in *d* and *f*. Null embryos also show remodeling defects of trunk arteries (arrowheads) and intersomitic vessels (open arrowheads) (*b*). LacZ reporter knocked into the *Tmem100* allele was used to visualize developing arteries, and the embryos heterozygous for the *Tmem100* null allele are shown as a control with normal vascular structure. cv, cardinal vein; da, dorsal aorta; en, endodermal layers; me, mesodermal layers; sv, sinus venosus. (Scale bars: *A*, *a–d*, 200 μm; *A*, *e* and *f*, and *B*, 50 μm; and *A*, *g* and *h*, 20 μm.)

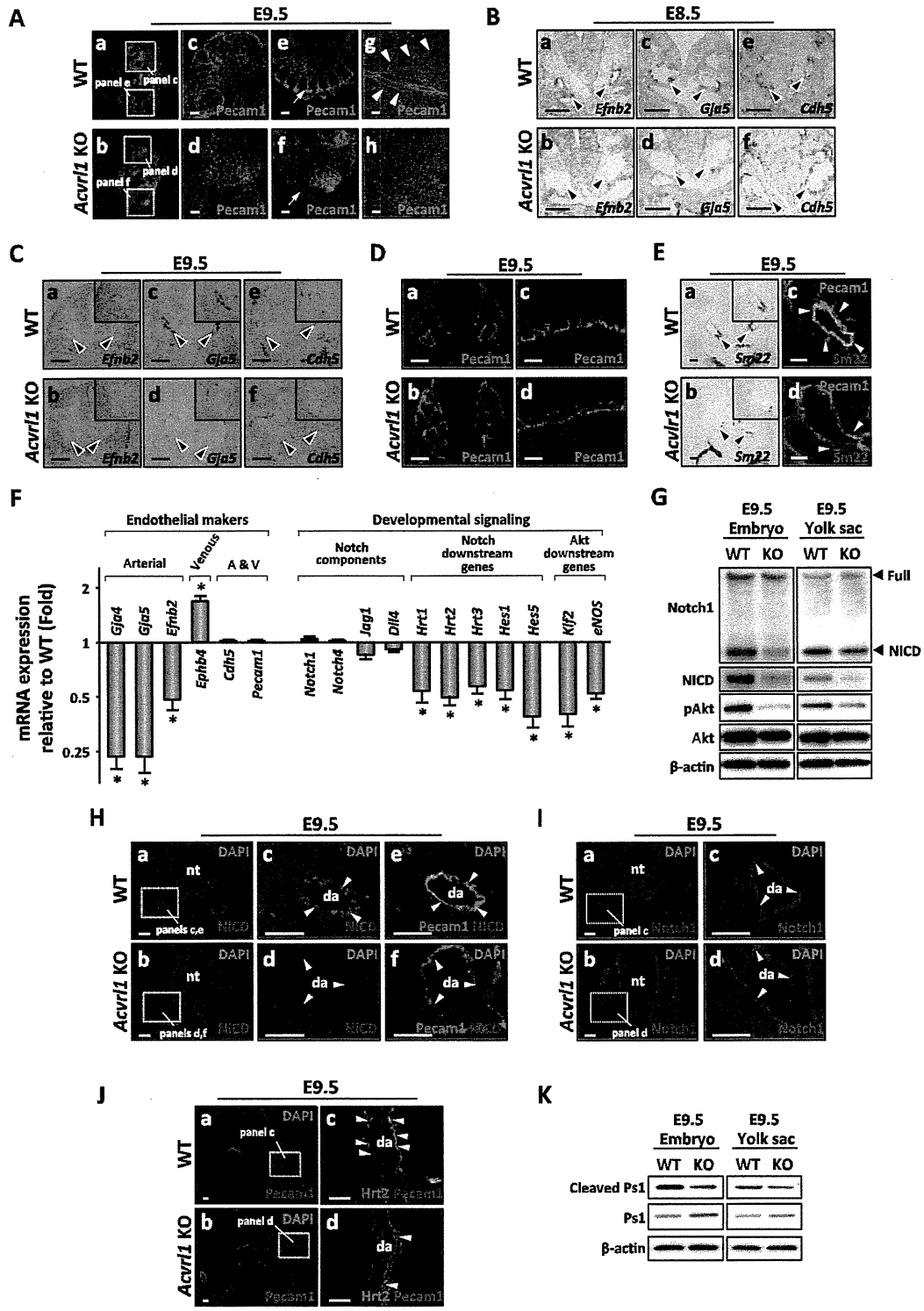

Fig. S6. Defects of arterial differentiation and dysregulation of Notch- and Akt-mediated signaling pathways in *Acvrl1/Alk1* null embryos. (*A*) Whole-mount Pecam1 immunostaining shows defects of vascular remodeling in the embryo proper (*b*, *d*, and *f*) and yolk sac (*h*) in *Acvrl1/Alk1* null mice. Arrows indicate intersomitic vessels. Arrowheads indicate a well-branched vascular tree in the yolk sac, which is observed only in wild-type mice. *a–f* are shown with nuclear DAPI stain. (*B* and *C*) Expression of arterial endothelium marker genes, *Efnb2* and *Gja5/Cx40*, diminishes in dorsal aorta of *Acvrl1/Alk1* null embryos (arrowheads in *b* and *d*) at E8.5 (*B*) and E9.5 (*C*). In contrast, the expression of *Cdh5*, which is detected both in the arteries and in the veins, is maintained (arrowheads in *f*). In situ hybridization is shown. (*D*) Expression of an endothelial marker, Pecam1, is maintained in dorsal aorta of an *Acvrl1/Alk1* null embryo (*b*) and in the yolk sac (*d*). Immunohistochemistry is shown. *a–d* are shown with nuclear DAPI stain. (*E*) Expression of *Sm22/Tagln* mRNA and Sm22 protein in the mural layers of dorsal aorta is significantly reduced in *Acvrl1/Alk1* null embryos (arrowheads). In situ hybridization (*a* and *b*) and immunohistochemistry (*c* and *d*) are shown. *Insets* in *C* and *E* show magnified views of dorsal aorta. *c* and *d* are shown with nuclear DAPI stain. (*F*) As in *Tmem100* null embryos, expression of arterial endothelium markers, Notch downstream genes, and Akt downstream genes shows significant reduction in *Acvrl1/Alk1* null yolk sacs at E9.5. In contrast,

Legend continued on following page

a venous endothelium marker *Ephb4* is significantly up-regulated. Quantitative RT-PCR is shown. (*G*) The amount of the intracellular domain of Notch receptor (NICD) and phosphorylated Akt significantly decreases in *Acvrl1/Alk1* null embryos and yolk sac at E9.5, whereas that of full-length Notch receptor and total Akt remains unchanged. Note that anti-Notch1 antibody detects full-length Notch receptors, cleavage intermediate protein(s), and NICD, whereas anti-NICD antibody recognizes only mature NICD protein. (*H*) NICD expression in endothelial cells of dorsal aorta (da) markedly decreases in *Acvrl1/Alk1* null embryos. NICD expression is shown with (*e* and *f*) or without (*c* and *d*) endothelial Pecam1 immunostaining. *a–f* are shown with nuclear DAPI stain. (*I*) Expression of full-length Notch receptors in the endothelium of dorsal aorta is unchanged in *Acvrl1/Alk1* null embryos. Immunohistochemistry is shown. *a–d* are shown with nuclear DAPI stain. (*J*) Expression of Hrt2, a Notch downstream transcription factor, in dorsal aorta significantly decreases in *Acvrl1/Alk1* null embryos. Immunohistochemistry is shown. *a* and *b* are shown with nuclear DAPI stain. (*K*) Cleaved Presenilin-1 (Ps1) decreases in *Acvrl1/Alk1* null embryos and yolk sac at E9.5. Western blot analysis is shown. (Scale bars: *A–C* and *D*, *a* and *b*, 50 μm; and *D*, *c* and *d*, *E*, and *H–J*, 20 μm.)

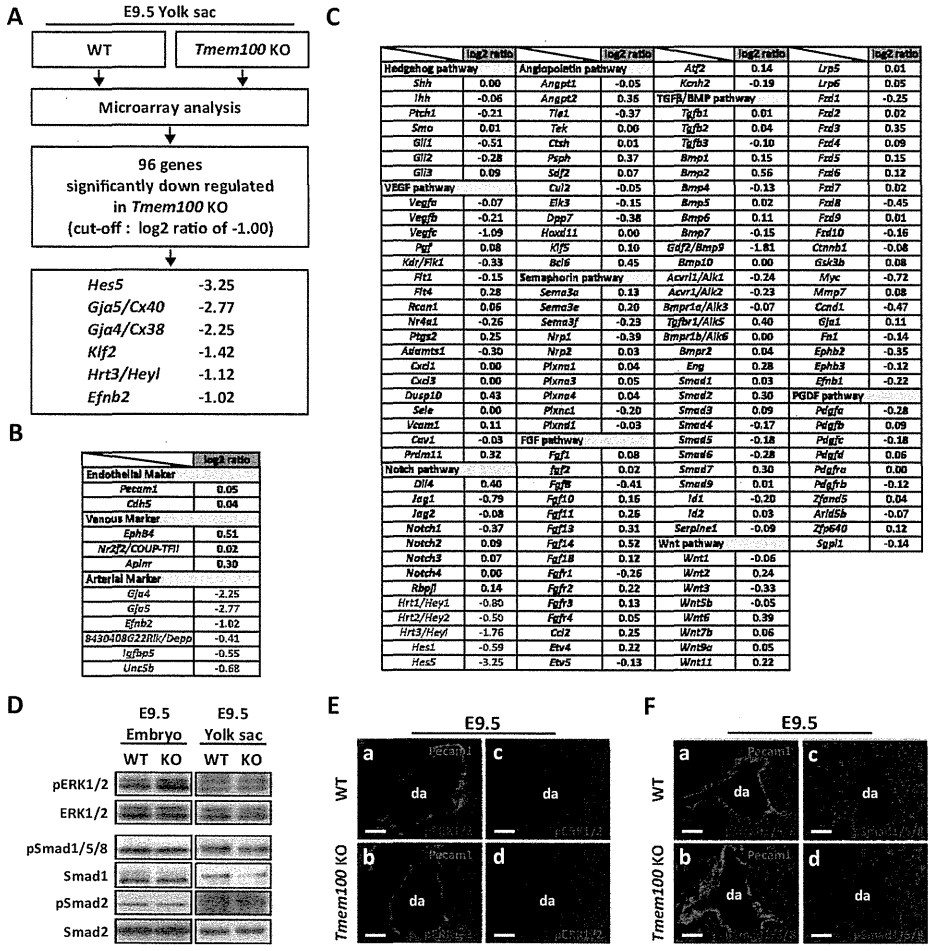

Fig. S7. Analysis of arterial endothelium differentiation and vascular signaling in *Tmem100* null yolk sac. (*A*) A microarray analysis was performed by using the yolk sac of wild-type (WT) and *Tmem100* null (KO) mice at E9.5. The list comprises down-regulated genes in *Tmem100* null yolk sac (cutoff: log2 ratio of +1.00). (*B* and *C*) Lists of microarray data (log2 ratio). Endothelial marker genes (*B*) and components of vascular signaling pathways and their downstream target genes (*C*) are shown. Markers of arterial endothelium differentiation and Notch target genes (highlighted in red) are significantly down-regulated. The results were confirmed by quantitative RT-PCR, as demonstrated in Fig. 4*A*. (*D–F*) Phosphorylation levels of ERK1/2 (*D* and *E*), Smad1/5/8 (*D* and *F*), and Smad2 (*D*) show no significant differences between wild-type and *Tmem100* null mice. Western blot analysis (*D*) and immunohistochemistry (*E* and *F*) are shown. (Scale bars in *E* and *F*, 10 μm.)

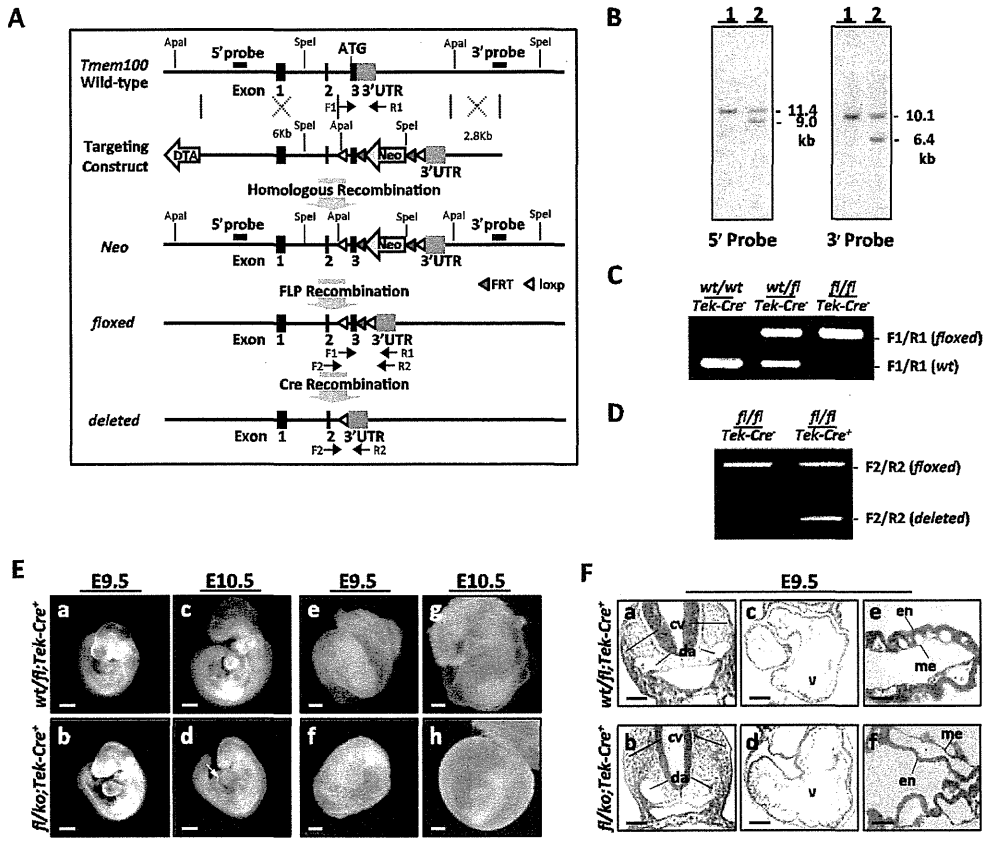

Fig. S8. Impairment of angiogenesis by endothelial-specific deletion of *Tmem100*. (*A*) Schematic diagram represents the conditional targeting of the *Tmem100* gene. (*B*) Southern blot analysis of control (lane 1) and $Tmem100^{wt/neo}$ (lane 2) ES cells. Positions of the 5′ and 3′ probes for Southern blot analysis are shown in *A*. (*C*) A representative result of PCR genotyping of mice from a $Tmem100^{wt/fl}$;*Tek-Cre*$^{-}$ × $Tmem100^{wt/fl}$;*Tek-Cre*$^{-}$ mating. (*D*) Cre-mediated recombination of the floxed *Tmem100* allele with the *Tek-Cre*$^{+}$ transgene in the yolk sac. Positions of PCR primers (F1, F2, R1, and R2) are shown in *A*. (*E*) Endothelial-specific *Tmem100* knockout embryos ($Tmem100^{fl/ko}$;*Tek-Cre*$^{+}$) show pericardial effusion (arrow) and severe growth retardation at E10.5. There are no major vitelline vessels in endothelial-specific *Tmem100* knockout yolk sac. (*F*) Impairment of cardiovascular morphogenesis is observed in endothelial cell-specific *Tmem100* knockout mice. As in global *Tmem100* null mice, paired dorsal aortas (da) are highly dilatated or narrow in $Tmem100^{fl/ko}$;*Tek-Cre*$^{+}$ embryos. Trabeculae of ventricular (v) myocardium are not well formed in $Tmem100^{fl/ko}$;*Tek-Cre*$^{+}$ embryos. Yolk sacs of endothelial-specific *Tmem100* knockout mice show large lacunae by a detachment of endodermal (en) and mesodermal (me) layers. H&E staining is shown. (Scale bars: *E*, 200 μm; *F*, *a*–*d*, 50 μm; and *F*, e and *f*, 20 μm.)

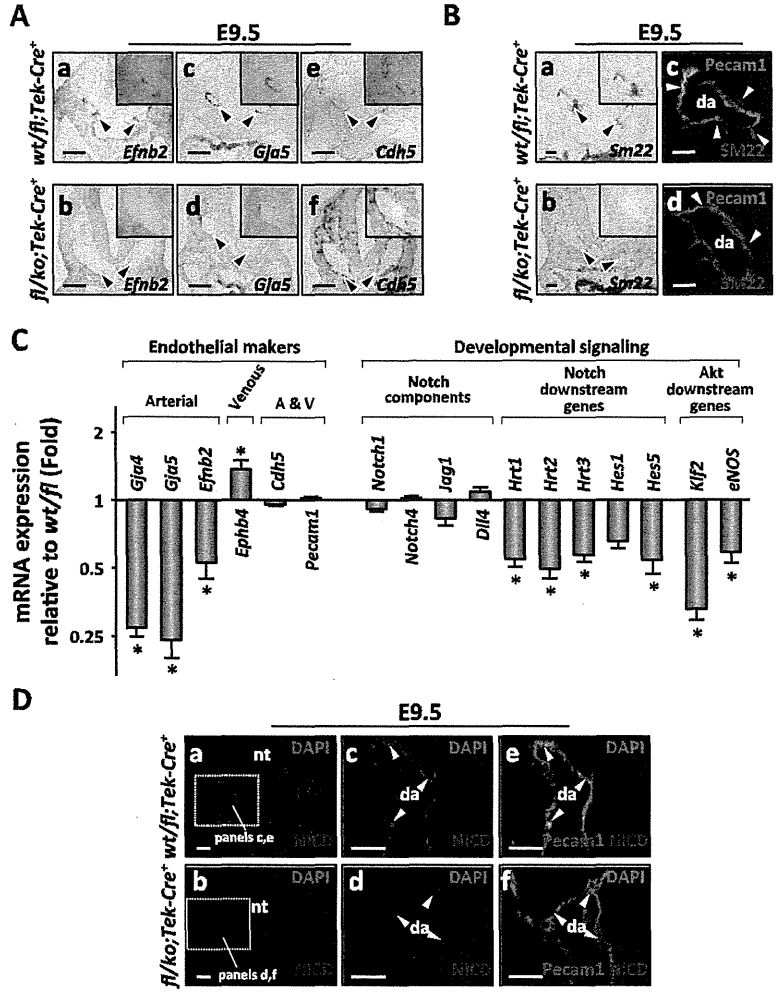

Fig. S9. Defects of arterial differentiation and dysregulation of Notch- and Akt-related signaling pathways in endothelial-specific *Tmem100* knockout mice. (*A*) Expression levels of arterial marker genes, *Efnb2* and *Gja5/Cx40*, decreased in dorsal aorta (arrowheads in *b* and *d*) of endothelial-specific *Tmem100* knockout embryos at E9.5, whereas *Cdh5* expression appears unaffected (*f*). In situ hybridization is shown. (*B*) mRNA and protein expression of a smooth muscle cell marker *Sm22/Tagln* is lost in the mural layers of dorsal aorta of endothelial-specific *Tmem100* knockout embryos. In situ hybridization (*a* and *b*) and immunohistochemistry (*c* and *d*) are shown. *c* and *d* are shown with nuclear DAPI stain. (*C*) Expression analysis of the yolk sac from endothelial-specific *Tmem100* knockout mice at E9.5. Expression of arterial endothelium markers and Notch/Akt-downstream genes is highly down-regulated, as in the global *Tmem100* null yolk sac. Quantitative RT-PCR is shown. (*D*) NICD expression markedly decreases in endothelial cells of dorsal aorta (da) in endothelial-specific *Tmem100* knockout embryos. NICD expression is shown with (*e* and *f*) or without (*c* and *d*) endothelial Pecam1 immunostaining. nt, neural tube. Immunohistochemistry is shown. *a–f* are shown with nuclear DAPI stain. (Scale bars: *A*, 50 μm; and *B* and *D*, 20 μm.)

Circulation Journal
Official Journal of the Japanese Circulation Society
http://www.j-circ.or.jp

ORIGINAL ARTICLE
Heart Failure

Urinary 8-Hydroxy-2'-Deoxyguanosine as a Novel Biomarker for Predicting Cardiac Events and Evaluating the Effectiveness of Carvedilol Treatment in Patients With Chronic Systolic Heart Failure

Takehisa Susa, MD; Shigeki Kobayashi, MD, PhD; Takeo Tanaka, MD, PhD; Wakako Murakami, MD; Shintaro Akashi, MD; Ichiro Kunitsugu, MD; Shinichi Okuda, MD, PhD; Masahiro Doi, MD, PhD; Yasuaki Wada, MD, PhD; Tomoko Nao, MD, PhD; Jutaro Yamada, MD, PhD; Takeshi Ueyama, MD, PhD; Takayuki Okamura, MD, PhD; Masafumi Yano, MD, PhD; Masunori Matsuzaki, MD, PhD

Background: The authors recently reported that urinary 8-hydroxy-2'-deoxyguanosine (U8-OHdG) derived from cardiac tissue reflects clinical status and cardiac dysfunction severity in patients with chronic heart failure (CHF). The aim of the present study was to investigate whether U8-OHdG levels can accurately predict cardiac events in CHF patients and their response to β-blocker treatment.

Methods and Results: Plasma brain natriuretic peptide (BNP) and U8-OHdG levels were measured in 186 consecutive CHF patients before discharge. Patients were then prospectively followed (median follow-up, 649 days) with endpoints of cardiac death or hospitalization due to progressive heart failure. From receiver operating characteristic curve analysis, cut-offs were 12.4 ng/mg creatinine (Cr) for U8-OHdG and 207 pg/ml for BNP. On multivariate Cox analysis, U8-OHdG and BNP were independent predictors of cardiac events. Patients were classified into 4 groups according to U8-OHdG and BNP cut-offs. The hazard ratio for cardiac events in patients with BNP ≥207 pg/ml and U8-OHdG ≥12.4 ng/mg Cr was 16.2 compared with approximately 4 for patients with only 1 indicator above its respective cut-off. Furthermore, carvedilol therapy was initiated in 30 CHF patients. In responders (≥10% increase in left ventricular ejection fraction [LVEF] or ≥1 class decrease in New York Heart Association [NYHA] class), U8-OHdG levels decreased significantly along with improved NYHA class, LVEF, and BNP levels after treatment.

Conclusions: U8-OHdG may be a useful biomarker for predicting cardiac events and evaluating β-blocker therapy effectiveness in CHF patients. (*Circ J* 2012; **76:** 117–126)

Key Words: Biomarker; Heart failure; Oxidative stress

Chronic heart failure (CHF) is characterized by hemodynamic abnormalities, neurohormonal activation, relentless progression, and high mortality.[1,2] CHF progresses through structural remodeling of the heart and likely involves neurohormonal activation.[3] Although previous studies have confirmed the prognostic importance of neurohormones such as brain natriuretic peptide (BNP), norepinephrine, interleukin-6 (IL-6), tumor necrosis factor-α (TNF-α), and angiotensin II (Ang II),[4–7] BNP has been found to be the most sensitive.[3] BNP and N-terminal proBNP are particularly useful for evaluating clinical symptoms and cardiac dysfunction and predicting prognosis in patients with CHF; this is because they are cardiac specific, because they are secreted from the ventricles according to volume and pressure overload.[8,9] Thus, they are the most well-established diagnostic and prognostic biomarkers for CHF patients.[10] Recent studies suggest that use of other biomarkers in combination with BNP may exhibit increased effectiveness for evaluating the pathogenesis of heart failure as well as the prognosis and risk stratification of patients with CHF.[11–13]

Inflammation, activation of the renin-angiotensin-aldosterone system and sympathetic nervous system, and increases in

Received May 26, 2011; revised manuscript received September 7, 2011; accepted September 8, 2011; released online October 19, 2011
Time for primary review: 24 days

Division of Cardiology, Department of Medicine and Clinical Science (T.S., S.K., T.T., W.M., S.A., S.O., M.D., Y.W., T.N., J.Y., T.U., T.O., M.Y., M.M.), Department of Public Health (I.K.), Yamaguchi University Graduate School of Medicine, Ube, Japan
Mailing address: Shigeki Kobayashi, MD, PhD, Division of Cardiology, Department of Medicine and Clinical Science, Yamaguchi University Graduate School of Medicine, 1-1-1 Minamikogushi, Ube 755-8505, Japan. E-mail: skoba@yamaguchi-u.ac.jp

ISSN-1346-9843 doi:10.1253/circj.CJ-11-0537

Table 1. Baseline Patient Characteristics With and Without Cardiac Events

	Total (n=186)	Event (–) (n=123)	Event (+) (n=63)	P value
Gender (M/F)	114/72	77/46	37/26	0.6356
Age (years)	56.7±14.8	57.1±13.6	55.8±17.0	0.5678
BMI (kg/m^2)	22.5±5.6	22.8±5.5	23.0±5.8	0.1110
NYHA class	2.0±0.8	1.8±0.7	2.5±0.9	<0.0001
U8-OHdG (ng/mg Cr)	13.1±6.0	11.8±5.2	15.7±6.5	<0.0001
U8-isoprostane (ng/mg Cr)	263.4±166.4	235.7±154.3	354.3±184.2	0.8147
Ang II (ng/ml)	25.4±35.3	25.4±39.8	25.5±13.6	0.9941
TNF-α (ng/ml)	2.0±3.2	2.0±3.5	2.0±1.9	0.9793
IL-6 (ng/ml)	4.3±4.5	4.1±4.5	4.6±4.7	0.6446
BNP (pg/ml)	369.7±450.4	268.7±315.9	566.7±590.8	<0.0001
FBS (mg/dl)	99.2±23.7	101.9±24.3	93.4±21.8	0.0707
HbA_{1c} (%)	6.3±1.4	6.4±1.6	6.1±0.9	0.7062
T-cho (mg/dl)	187.4±42.8	190.0±45.1	182.0±37.2	0.3521
Triglycerides (mg/dl)	124.7±67.0	132.5±71.1	101.5±47.4	0.0736
LDL-C (mg/dl)	120.1±40.1	120.9±41.5	116.4±35.3	0.7509
Cr (mg/dl)	1.06±0.52	0.95±0.34	1.28±0.71	0.0067
eGFR (ml/min)	62.7±27.1	66.4±26.2	55.4±27.7	0.0049
Uric acid (mg/dl)	7.2±2.3	6.8±2.0	7.8±2.8	0.0058
TBil (mg/dl)	0.9±0.6	0.9±0.5	0.9±0.6	0.9533
hsCRP (mg/dl)	0.37±0.59	0.32±0.55	0.49±0.66	0.0155
SBP (mmHg)	99.7±17.4	104.0±17.1	90.9±14.5	<0.0001
Heart rate (beats/min)	74.7±13.1	74.9±13.7	74.4±11.8	0.8260
LVDD (mm)	63.3±8.7	62.6±8.7	64.7±8.6	0.1221
LVEDVI (ml/m^2)	128.8±47.3	124.0±45.6	137.1±49.3	0.0793
LVEF (%)	28.5±8.4	29.4±8.2	26.6±8.4	0.0306
Treatment				
β-blocker	83 (155)	80 (98)	90 (57)	0.0651
ACEI/ARB	87 (162)	87 (107)	87 (55)	>0.9999
Loop diuretics	78 (146)	72 (88)	92 (58)	0.0012
Aldosterone antagonist	51 (94)	46 (56)	60 (38)	0.0875
Statin	27 (50)	25 (31)	30 (19)	0.4906

Data given as mean±SD or % (n).
BMI, body mass index; NYHA, New York Heart Association; U8-OHdG, urinary 8-OHdG; U8-isoprostane, urinary 8-isoprostane; U8-isoprostane, urinary 8-isoprostane; Ang II, angiotensin-II; TNF-α, tumor necrosis factor-α; IL-6, interleukin-6; BNP, B-type natriuretic peptide; FBS, fasting blood sugar; HbA_{1c}, hemoglobin A_{1c}; T-cho, total cholesterol; LDL-C, low-density lipoprotein cholesterol; Cr, serum creatinine; eGFR, estimated glomerular filtration rate; TBil, total bilirubin; hsCRP, high-sensitivity C-reactive protein; SBP, systolic blood pressure; LVDD, left ventricular end-diastolic diameter; LVEDVI, left ventricular end-diastolic volume index; LVEF, left ventricular ejection fraction; ACEI, angiotensin-converting enzyme inhibitors; ARB, angiotensin receptor blockers.

circulating catecholamine levels and peroxynitrite formed from interactions between superoxide anion and nitric oxide may all increase oxidative stress.[14] Several studies have evaluated the potential utility of plasma myeloperoxidase, plasma oxidized low-density lipoproteins (oxidized LDL), serum/urinary isoprostane, urinary biopyrrins, uric acid, and markers of nitro-redox imbalances such as *S*-nitrosohemoglobin, nitric oxide, and nitrite for evaluation of CHF severity and prognosis.[15–23] An oxidized nucleoside of DNA, 8-hydroxy-2'-deoxyguanosine (8-OHdG), is also reported to be a sensitive biomarker for oxidative DNA damage in vivo.[24–26] It is reported that the production of reactive oxygen species (ROS) results in mitochondrial DNA damage as evaluated with 8-OHdG in mice with failing hearts after myocardial infarction.[27,28] Furthermore, 8-OHdG can also be detected immunohistochemically in human cardiac tissue in patients with severe dilated cardiomyopathy (DCM).[29] Recently, we reported that 8-OHdG is produced in failing cardiac tissue on the basis of sampling data from the coronary sinus and aortic root.[30] In addition, the urinary excretion of 8-OHdG is significantly correlated with clinical status and cardiac dysfunction in patients with CHF.[30] Thus, urinary (U) 8-OHdG may be a useful cardiac biomarker for evaluating oxidative stress at the cellular level and predicting the outcome of patients with CHF. In the present study, we investigated whether U8-OHdG is a clinically useful biomarker for predicting the morbidity and mortality of patients with CHF compared with plasma BNP – the current gold standard biomarker for heart failure – and other neurohumoral factors. We also examined whether a combination of plasma BNP and U8-OHdG can reliably be used to stratify the risk of CHF patients for cardiac events.

Methods

Subjects and Study Protocol

One hundred and eighty-six consecutive patients with left ven-

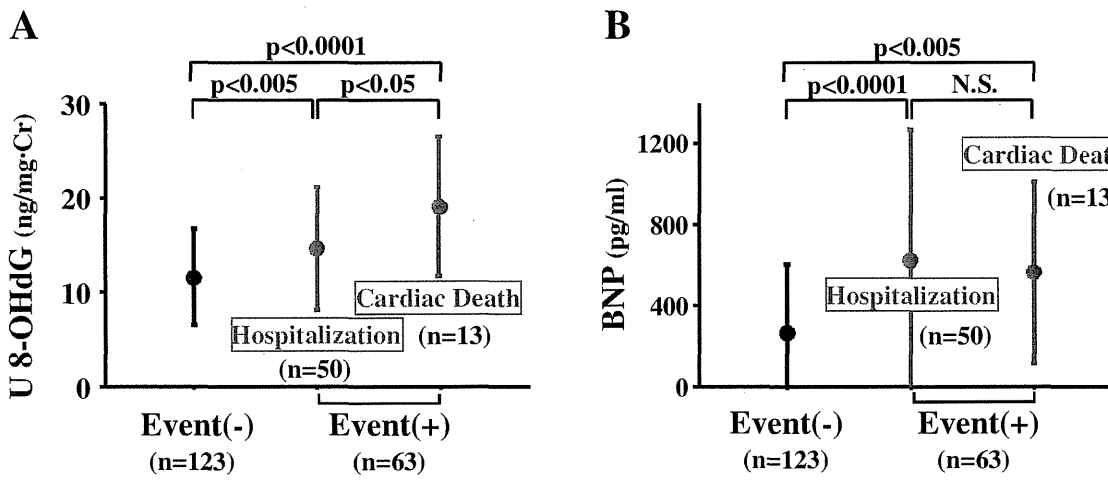

Figure 1. Comparison of (**A**) urinary 8-hydroxy-2'-deoxyguanosine (U8-OHdG) and (**B**) plasma brain natriuretic peptide (BNP) in patients with and without cardiac events (hospitalization or cardiac death).

tricular (LV) dysfunction (LV ejection fraction [LVEF] <45%) who had received standard medication, including β-blockers, angiotensin-converting enzyme inhibitors (ACEI), angiotensin receptor blockers (ARB), diuretics, and aldosterone antagonist for >3 months were enrolled in the present study at Yamaguchi University Hospital between June 2005 and June 2010; 135 of these patients were diagnosed with idiopathic DCM; 17 with secondary cardiomyopathy excluding restrictive cardiomyopathy, myocarditis, and cardiac sarcoidosis (ie, hypertensive heart disease, valvular heart disease, or diabetic cardiomyopathy); and 34 with old myocardial infarction (OMI). DCM was diagnosed according to the criteria of the 1995 World Health Organization/International Society and Federation of Cardiology Task Force.[31] Secondary cardiomyopathy was diagnosed according to clinical history, physical examination, electrocardiogram, echocardiography, and cardiac catheterization including endomyocardial biopsy. OMI was defined as revascularization >3 months previously and no ischemic region in the LV on coronary angiography and/or adenosine-induced myocardial perfusion scintigraphy. All CHF patients were enrolled during steady state within 7 days before discharge. Patients with a smoking habit, acute coronary syndrome, acute myocarditis, severe renal failure, cancer, or inflammatory diseases such as infection or collagen disease were excluded from the study irrespective of CHF severity; this is because oxidative stress has been shown to be increased in these systemic diseases.

Heart failure severity was evaluated on New York Heart Association (NYHA) class, echocardiography, and/or cardiac catheterization; moreover, we collected morning urine samples to measure the concentrations of U8-OHdG and U8-isoprostane as oxidative stress markers and collected blood samples from peripheral veins for blood biochemistry and to evaluate BNP, IL-6, Ang II, TNF-α, and high-sensitivity C-reactive protein (hsCRP) levels. Blood was centrifuged at 3,000 rpm for 15 min at 4°C, and the plasma was frozen in aliquots and stored at –80°C until assaying. Morning urine was also frozen in aliquots and stored at –80°C until assaying. The CHF patients were prospectively followed for a median follow-up period of 649 days, with endpoints of cardiac death or hospitalization due to progressive heart failure.

A total of 186 patients received standard medications, including ACEI, β-blockers, digitalis, and diuretics (**Table 1**).

Informed consent was obtained from all patients before participation in the study. The protocol was approved by the Human Investigations Committee of Yamaguchi University Hospital and conformed to the Declaration of Helsinki.

Endpoints and Follow-up

No patients were lost to follow-up (median follow-up, 649±505 days) after discharge. Events were centrally adjudicated using medical records, autopsy reports, and death certificates. The first endpoint was defined as cardiac death from worsening heart failure or sudden cardiac death, and the second endpoint was defined as worsening heart failure requiring readmission. Sudden cardiac death was defined as death without definitive premonitory symptoms or signs and was established by the attending physician.

Comparison of U8-OHdG Levels Before and After Carvedilol Treatment

To investigate whether U8-OHdG is useful for evaluating the effectiveness of β-blocker therapy in patients with CHF, 30 consecutive patients who had received standard medication such as diuretics, ACEI/ARB, or aldosterone antagonists, but who had not received β-blocker medications were selected for the present study. A responder was defined as a patient showing clinical improvement of either ≥10% in LVEF or ≥1 class of NYHA functional classification after treatment with a β-blocker. After treatment with β-blockers (mean follow-up period, 12 months), NYHA class, LVEF on echocardiography, BNP, IL-6, Ang II, TNF-α, hsCRP, and U8-OHdG were re-examined to evaluate their usefulness as oxidative stress biomarkers compared with plasma BNP (the gold standard biomarker of heart failure), and the aforementioned neurohumoral and inflammatory biomarkers.

Measurement of U8-OHdG and Other Neurohumoral and Inflammatory Factors

Serum TNF-α and IL-6 levels were determined using the Quantikine HS (Quantikine HS; R&D Systems, Minneapolis, MN,

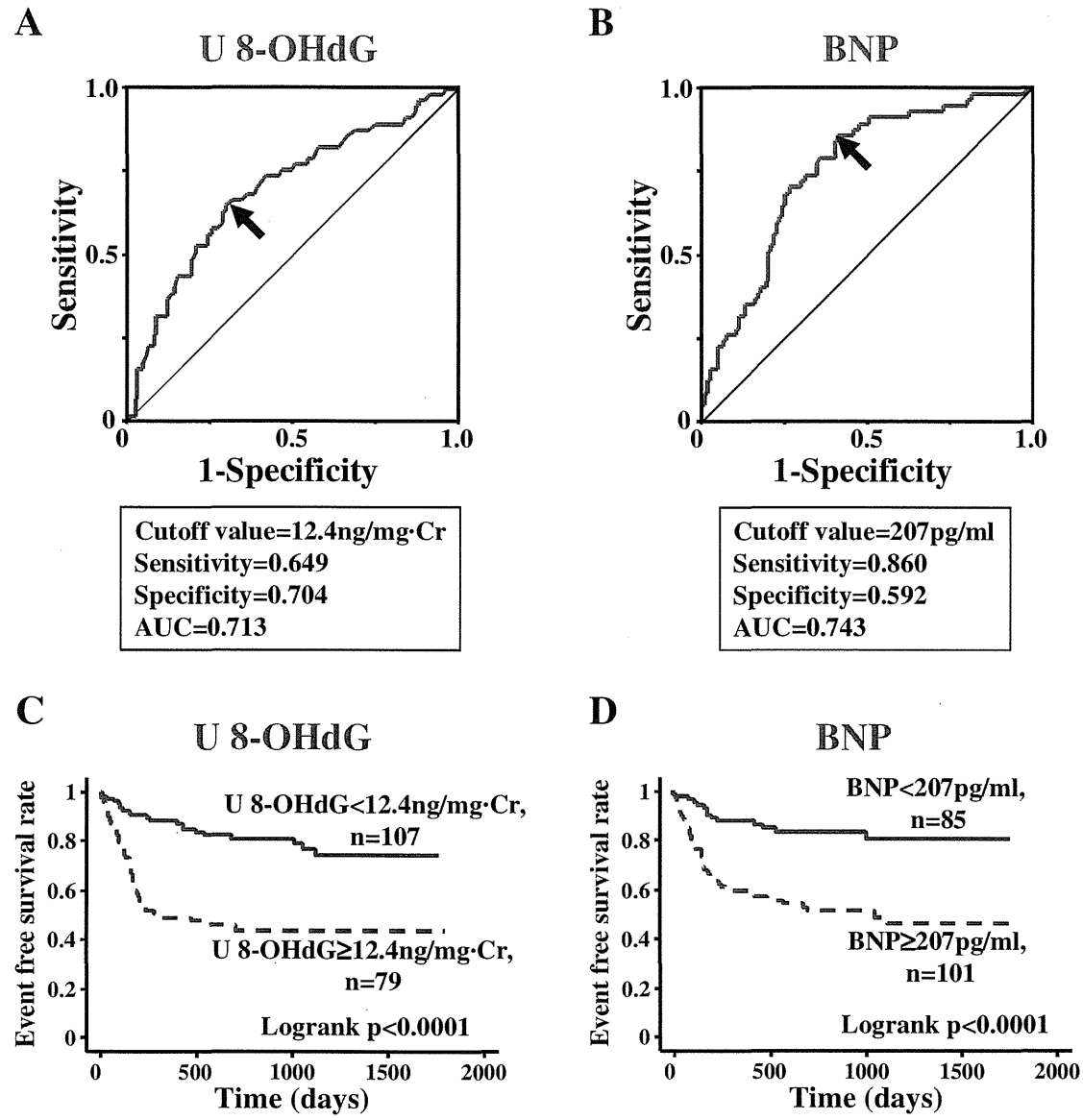

Figure 2. Receiver operating characteristic analysis of (**A**) urinary 8-hydroxy-2'-deoxyguanosine (U8-OHdG) and (**B**) plasma brain natriuretic peptide (BNP). Kaplan-Meier event-free curves for patients with chronic heart failure divided into 2 groups based on cut-off levels for (**C**) urinary 8-OHdG and (**D**) plasma BNP. AUC, area under the curve.

USA) and CLEIA (Fujirebio, Tokyo, Japan) immunoassays.[32]

Plasma Ang II levels were measured using a radioimmunoassay with a specific antibody directed against synthetic Ang II as described previously.[33] U8-OHdG levels were measured using a commercially available ELISA kit (Japan Institute for the Control of Aging, Fukuroi, Japan). U8-isoprostane was also determined using an 8-isoprostane EIA kit (Cayman Chemical, Ann Arbor, MI, USA). Raw data were normalized to the urinary level of creatinine (Cr). Plasma BNP was measured using the Shionoria BNP Kit (Shionogi Pharmaceutical, Osaka, Japan). Echocardiographic evaluation was performed by independent echocardiologists. LVEF and cardiac volumes were measured using the Simpson biplane method.

Statistical Analysis

Descriptive statistics for continuous variables are expressed as mean±SD. Student's t-test was used to compare continuous variables between genders. The chi-square test was used to compare prevalence or frequencies. Cut-offs were defined by the point of maximum sensitivity+specificity upon receiver operating characteristic (ROC) analysis. Kaplan-Meier analysis was performed on the cumulative rates of cardiac event-free status in patients with CHF who were divided into 2 groups on the basis of cut-offs for BNP, U8-OHdG, U8-isoprostane, or uric acid. Differences between cardiac event-free curves were analyzed using the log-rank test. To identify independent cardiac event predictors, we initially performed univariate and multivariate analyses with Cox's proportional

Table 2. Risk Factors for Cardiac Events in CHF Patients

	Univariate		Multivariate (model 1)		Multivariate† (model 2)	
	HR (95%CI)	P value	HR (95%CI)	P value	HR (95%CI)	P value
Age	0.993 (0.976–1.010)	0.417	0.946 (0.866–1.032)	0.210	0.945 (0.910–0.982)	0.004
Gender	0.828 (0.500–1.372)	0.464	0.148 (0.026–0.855)	0.033		
SBP	0.950 (0.929–0.971)	<0.0001	0.934 (0.886–0.984)	0.011	0.934 (0.902–0.967)	<0.0001
HR	1.000 (0.979–1.021)	1.000	1.033 (0.952–1.119)	0.436		
NYHA						
Grade 1	Reference		Reference			
Grade 2	1.875 (0.845–4.160)	0.122	0.355 (0.041–3.098)	0.349		
Grade 3	4.970 (2.171–11.377)	<0.0001	0.251 (0.013–4.860)	0.360		
Grade 4	13.920 (5.454–35.529)	<0.0001	13.132 (0.069–2,502.927)	0.336		
U8-OHdG	1.071 (1.037–1.106)	<0.0001	1.110 (0.913–1.349)	0.295	1.161 (1.076–1.253)	<0.0001
U8-isoprostane	1.000 (0.998–1.002)	0.947	1.001 (0.996–1.006)	0.704		
BNP	1.001 (1.001–1.002)	<0.0001	1.003 (1.000–1.005)	0.030	1.002 (1.001–1.003)	<0.0001
Ang II	1.001 (0.991–1.011)	0.881	1.006 (0.975–1.038)	0.723		
IL-6	1.042 (0.964–1.126)	0.303	1.247 (0.909–1.711)	0.171		
Uric acid	1.166 (1.057–1.286)	0.002	0.944 (0.670–1.330)	0.741		
CRP	1.354 (0.966–1.898)	0.079	0.957 (0.710–1.289)	0.770		
Sodium	0.824 (0.765–0.888)	<0.0001	1.018 (0.979–1.058)	0.366		
eGFR	0.985 (0.974–0.996)	<0.0001	1.030 (0.996–1.065)	0.082		
LVEDVI	1.004 (0.999–1.009)	0.105	1.104 (0.937–1.302)	0.937		
LVEF	0.968 (0.939–0.998)	0.039	1.030 (0.952–1.302)	0.238		

CHF, chronic heart failure; HR, hazard ratio; CI, confidence interval; CRP, C-reactive protein. Other abbreviations see in Table 1.
†Cox proportional model 2 was developed using the stepwise downward method.

hazard model in which we included 16 confounding factors. To refine the models with fewer parameters, we used the step-down method. We adopted Cox's proportional hazard models to estimate hazard ratios (HR) and their 95% confidence intervals for each factor and to adjust for the effects of confounding factors. P-values were 2-sided, and P<0.05 was considered significant. Statistical analysis was done using SPSS 16.0J (SPSS Japan, Tokyo, Japan).

Results

Baseline CHF Patient Characteristics

Table 1 summarizes the baseline characteristics of the patients with and without cardiac events. A total of 186 patients with CHF were enrolled in the present study. During the mean follow-up period of 649 days, 63 patients had cardiac events (13 patients died due to worsening heart failure rather than sudden cardiac death, and 50 patients were admitted to hospital for decompensated heart failure; Figure 1). There were no differences with respect to gender, age, body mass index, U8-isoprostane, TNF-α, IL-6, fasting blood sugar, hemoglobin A_{1c}, total cholesterol, triglycerides, LDL cholesterol, total bilirubin, heart rate, LV end-diastolic dimension (LVDD), LV end-diastolic volume index (LVEDVI), or treatment with standard medications other than diuretics between the groups with and without cardiac events. But NYHA class, U8-OHdG, Ang II, plasma BNP, serum Cr, uric acid, and hsCRP were significantly higher and systolic blood pressure (SBP), LVEF, and estimated glomerular filtration rate (eGFR) were significantly lower in the group with cardiac events compared to the group without cardiac events.

Comparison of U8-OHdG and BNP Levels Between Groups

The levels of both U8-OHdG and BNP were significantly higher in patients with cardiac events than in those without (Table 1). After dividing the patients with cardiac events into 2 groups (ie, hospitalization and cardiac death), we compared these groups in terms of plasma BNP and U8-OHdG levels to clarify their clinical implications (Figure 1). U8-OHdG levels in the cardiac death group were significantly higher than those in the hospitalization group (cardiac death, 19.1±7.4 ng/mg Cr vs. hospitalization, 14.8±6.9 ng/mg Cr, P=0.0346), while there was no significant difference in the plasma BNP levels between the 2 groups (cardiac death, 555.0±404.8 pg/ml vs. hospitalization, 569.8±633.7 pg/ml).

Optimal Cut-off Values for Plasma BNP and U8-OHdG

The optimal cut-off values for BNP and U8-OHdG were set at the point of maximum sensitivity plus specificity on each ROC curve. The cut-off level was 12.4 ng/mg Cr for U8-OHdG with a sensitivity of 64.9% and a specificity of 70.4%, and 207 pg/ml for BNP with a sensitivity of 86.0% and a specificity of 59.2% (Figures 2A,B).

Univariate and Multivariate Analysis of Cardiac Events

We performed linear univariate and multivariate analyses of cardiac events for 16 variables (age, gender, SBP, heart rate, NYHA, U8-OHdG, U8-isoprostane, BNP, Ang II, IL-6, uric acid, hsCRP, sodium, eGFR, LVEDVI, and LVEF) to identify independent predictors of cardiac events (Table 2). Univariate analysis indicated that SBP, NYHA, U8-OHdG, BNP, uric acid, sodium, eGFR, and LVEF were significant predictors. Multivariate analysis identified high levels of SBP (P<0.0001), plasma BNP (P<0.0001), and U8-OHdG (P<0.0001) as significant independent predictors for cardiac events (Table 2).

Kaplan-Meier Analysis for Plasma BNP and U8-OHdG

Kaplan-Meier analysis was performed to evaluate the cumulative rates of cardiac event-free status in patients with CHF who were divided into 2 groups on the basis of cut-offs for BNP or U-8-OHdG. It was found that patients with values above the cut-off level had higher cardiac event rates than

Table 3. Clinical Characteristics of the 4 Groups of CHF Patients

	Low U8-OHdG		High U8-OHdG	
	Low BNP	High BNP	Low BNP	High BNP
n	50	57	35	44
Gender (M/F)	28/22	38/19	24/11	24/20
Age (years)	53.7±14.2	56.7±14.5	55.3±15.9	61.2±14.2*
BMI (kg/m^2)	23.9±6.4	22.4±4.7	23.9±7.2	20.0±2.9*,†
NYHA class	1.5±0.5	2.0±0.6*	2.0±0.8*	2.7±0.8*,†
U8-OHdG (ng/mg Cr)	9.3±2.0	9.1±2.1	17.6±5.0*,†	19.2±5.5*,†
U8-Isoprostane (ng/mg Cr)	198.2±66.7	228.3±158.9*	307.5±239.8*	480.0±118.6*
Ang II (pg/ml)	21.3±19.3	21.2±29.6	26.4±27.4	41.4±64.1†
TNF-α (pg/ml)	2.6±5.4	1.9±1.9	1.4±0.8	1.8±0.7
IL-6 (pg/ml)	3.4±3.2	5.1±5.6	2.7±1.8	5.8±5.5
BNP (pg/ml)	75.6±54.6	564.6±379.5*	91.7±58.1†	672.3±609.5*
FBS (mg/dl)	103.1±34.9	106.7±42.3	102.3±25.4	96.1±24.7
HbA_{1c} (%)	6.0±0.8	6.9±1.7*	6.3±2.1	5.8±0.7
T-cho (mg/dl)	199.5±42.4	185.3±46.8	172.3±36.8*	185.1±39.0
Triglycerides (mg/dl)	136.7±84.3	109.1±45.3	142.3±73.8	113.8±51.8
Cr (mg/dl)	0.88±0.28	1.05±0.45*	0.95±0.32	1.37±0.77*
eGFR (ml·min^{-1}·1.73m^{-2})	70.9±29.1	61.7±24.9	65.8±17.5	52.1±30.8*,†
Uric acid (mg/dl)	6.7±1.9	7.4±2.5	6.8±2.3	7.6±2.6
Sodium (mEq/L)	137.9±3.4	137.0±3.7	138.6±2.6	138.4±3.3
T-bil (mg/dl)	0.8±0.4	1.0±0.6	1.0±0.4*	0.9±0.7
hsCRP (mg/dl)	0.16±0.16	0.41±0.55*	0.38±0.80	0.55±0.70*
SBP (mmHg)	107.6±16.2	99.2±19.4*	100.4±11.6*	90.1±15.2*,†
Heart rate (beats/min)	70.1±10.6	76.8±13.6*	76.6±14.3*	75.7±13.0*
LVDD (mm)	60.0±7.3	64.8±8.8*	61.4±7.8	64.5±8.3*
LVEF (%)	33.6±7.4	26.7±7.8*	29.8±9.2*	25.4±7.0*
Treatment				
β-blocker	88 (44)	81 (46)	89 (31)	77 (34)
ACEI/ARB	92 (46)	84 (48)	86 (30)	86 (38)
Loop diuretics	74 (37)	79 (45)	74 (26)	86 (38)
Aldosterone antagonist	52 (26)	44 (25)	57 (20)	52 (23)
Statin	26 (13)	21 (12)	37 (13)	27 (12)

Data given as mean±SD or % (n).
Abbreviations see in Table 1.
*P<0.05 vs. the group with low U8-OHdG (<12.4 ng/mg Cr) and low BNP (<207 pg/ml); †P<0.05 vs. the group with low U8-OHdG (<12.4 ng/mg Cr) and high BNP (≥207 pg/ml).

those below the cut-off (**Figures 2C,D**).

Cardiac Event Prediction Stratified by a Combination of BNP and U8-OHdG

Patients were stratified into 4 groups according to combinations of cut-off levels of BNP and U8-OHdG (**Table 3**; **Figure 3A**). There were no significant differences in gender among the 4 groups. The HR of patients with high BNP and low U8-OHdG, low BNP and high U8-OHdG, and high BNP and high U8-OHdG were 4.2 (P=0.0101), 4.3 (P=0.0133), and 16.2 (P<0.0001), respectively, compared to those with low BNP and low U8-OHdG (**Figure 3B**).

Effectiveness of Carvedilol in CHF Patients According to U8-OHdG

Table 4 lists the characteristics of the 30 patients with CHF divided into responder and non-responder groups to carvedilol therapy. After carvedilol treatment, heart rate, LVDD, LVEDVI, BNP, and U8-OHdG decreased with an improvement in LVEF or NYHA class in the responder group but not in the non-responder group. In the responders and non-responders, the maximum dosage of carvedilol during the follow-up period was 11.9±7.1 mg/day and 7.4±6.3 mg/day, respectively. In the non-responders, the dose of carvedilol could not be increased due to adverse effects such as hypotension and worsening cardiac function compared to the responders. In the profiles based on the combined cut-off levels for U8-OHdG and BNP, the statuses of most of the responder patients moved to "low U8-OHdG and low BNP" (**Figure 4A**) after carvedilol treatment, whereas those of most of the non-responder patients did not (**Figure 4B**).

Discussion

The most important finding of the present study is that U8-OHdG is an oxidative stress biomarker that can be used to predict morbidity and mortality; it improves the prediction of cardiac events in combination with plasma BNP in patients with CHF as supported by the following findings. Based on ROC analysis, the cut-off values for U8-OHdG and BNP were determined to be 12.4 ng/mg Cr and 207 pg/ml, respectively. Kaplan-Meier analysis demonstrated that the high U8-OHdG group had a significantly higher incidence of cardiac events than the low U8-OHdG group, as was the case with BNP. Mul-

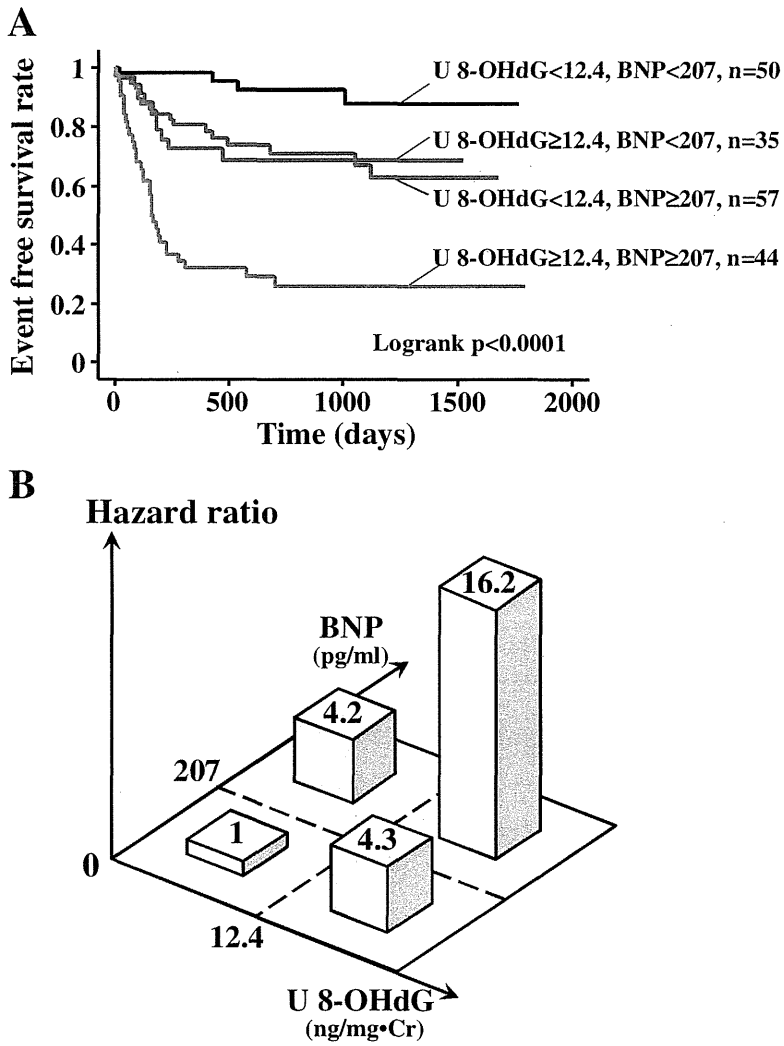

Figure 3. (A) Kaplan-Meier event-free curves for patients with chronic heart failure stratified into 4 groups based on cut-off levels for a combination of plasma brain natriuretic peptide (BNP) and urinary 8-hydroxy-2'-deoxyguanosine (U8-OHdG). (B) Hazard ratios for cardiac events in 4 groups based on cut-off levels for a combination of plasma BNP and U8-OHdG. There were significant differences between the reference group (low U8-OHdG and low BNP) and the other groups: 4.2 for low U8-OHdG and high BNP (P=0.0101), 4.3 for high U-8-OHdG and low BNP (P=0.0133), and 16.2 for high U8-OHdG and high BNP (P<0.0001).

Table 4. Changes in Clinical Outcomes After Carvedilol Treatment

	Responder group (n=19)			Non-responder group (n=11)		
	Before	After	P value	Before	After	P value
Age (years)	48±16			55±14		
Gender (M/F)	9/10			6/5		
BMI (kg/m^2)	24.5±7.9			23.1±8.7		
NYHA functional class	2.8±0.4	1.6±0.5	<0.0001	2.5±0.7	3.0±0.9	0.1245
Heart rate (beats/min)	81±17	71±8	0.0325	71±8	74±12	0.6319
SBP	99±22	96±16	0.7638	93.1±11	88±9	0.3293
T-Cho (mg/dl)	182±33	177±30	0.7620	183±31	195±23	0.5697
FBS (mg/dl)	107±57	105±29	0.9449	104±39	114±29	0.6522
LVDD (mm)	66±9	58±7	0.0048	64±7	64±9	0.7951
LVEDVI (ml/m^2)	140±46	105±30	0.0156	143±46	145±59	0.9266
LVEF (%)	23±5	36±13	0.0005	27±10	23±10	0.3847
eGFR (ml·min^{-1}·1.73m^{-2})	79±29	69±28	0.3317	60±27	50±28	0.4026
hsCRP (mg/dl)	0.38±0.38	0.14±0.19	0.0734	0.40±0.30	0.51±0.70	0.6859
BNP (pg/ml)	410±295	121±120	0.0003	424±399	571±783	0.5847
U8-OHdG (ng/mg Cr)	15.9±6.9	9.8±3.2	0.0013	13.4±6.3	20.3±4.4	0.0074
Follow-up period (days)		342±340			577±507	
β-blocker dose (mg)		11.9±7.1			7.4±6.3	

Data given as mean±SD or % (n).
Abbreviations see in Tables 1,2.

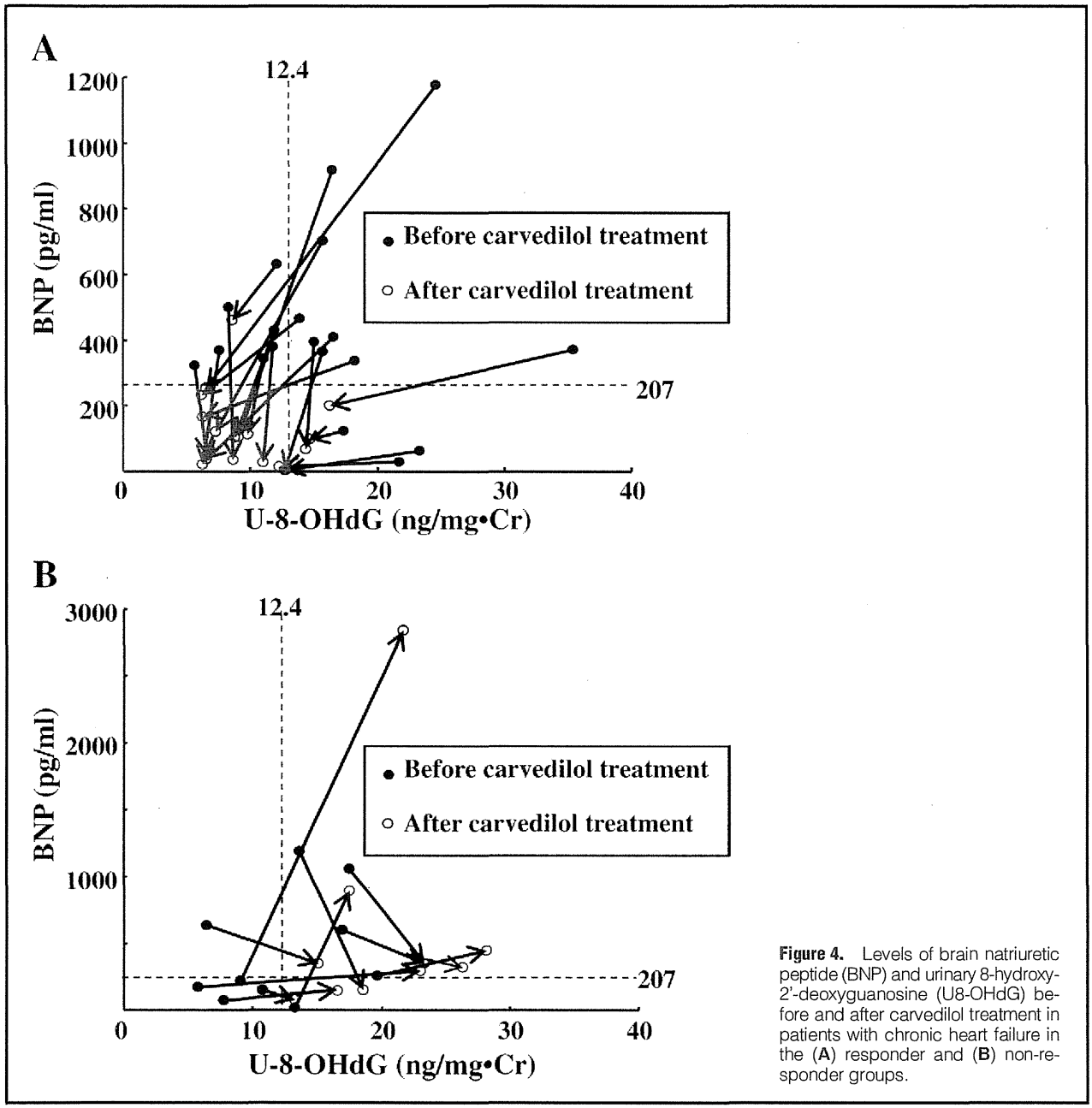

Figure 4. Levels of brain natriuretic peptide (BNP) and urinary 8-hydroxy-2'-deoxyguanosine (U8-OHdG) before and after carvedilol treatment in patients with chronic heart failure in the (**A**) responder and (**B**) non-responder groups.

tivariate analysis showed that U8-OHdG and BNP were independent predictors of cardiac events. Patients were stratified into 4 groups on the basis of the cut-off levels for both U8-OHdG and BNP (Table 3). Patients exceeding only 1 cut-off level had an HR of 4.2–4.3, while patients exceeding both cut-off levels had an HR of 16.2. Thus, a tandem approach using both BNP and U8-OHdG provides additional risk stratification and a better representation of the status of heart failure by evaluating the aspects of both wall stress and oxidative stress.

U8-OHdG as a Predictor of Cardiac Death in CHF Patients

U8-OHdG levels in the cardiac death group were significantly higher than those in the hospitalization group; meanwhile, there was no difference in plasma BNP levels between the 2 groups (Figure 1). Moreover, in all patients in the cardiac death group, U8-OHdG levels remained high during the follow-up period (data not shown). Thus, a high U8-OHdG level may be a more accurate predictor of cardiac death than BNP level in patients with CHF.

Clinical Implications

There are several advantages of using U8-OHdG as a biomarker for oxidative stress. First, 8-OHdG is partially produced in the failing myocardium;[27–30] thus, U8-OHdG may closely reflect clinical severity with respect to both symptoms and cardiac dysfunction in CHF.[17] Second, U8-OHdG is predictive of morbidity and mortality in patients with CHF; the HR for cardiac events markedly increased when the cut-off levels for both U8-OHdG and plasma BNP were exceeded.

It is reported that β-blockers and renin-angiotensin-aldosterone blockers both inhibit LV remodeling and improve the prognosis of patients with CHF, partly due to their antioxida-

tive stress effects.[34–39] Therefore, the present data demonstrate the possibility of treatment guided by both BNP and U8-OHdG as clinical biomarkers (Table 4, Figure 4).

Study Limitations

There were 2 significant limitations of the present study. First, this study was a single-center study; only a small number of subjects were analyzed, and only a small number of cardiac events occurred. A larger study is warranted to confirm the prediction of cardiac events according to U8-OHdG levels in patients with CHF. Second, we observed a consistent change in U8-OHdG levels with respect to the response to carvedilol therapy in 30 CHF patients. We could not clarify, however, whether the antioxidant action was a result of the radical scavenging action of carvedilol or the class effects of β-blockers. Further studies are needed to evaluate the efficacy of other β-blockers such as bisoprolol.

Conclusions

U8-OHdG is a useful oxidative stress biomarker for predicting cardiac events in patients with CHF, and substantially enhances the prediction of cardiac events when used in combination with BNP. Furthermore, U8-OHdG has the potential to be a potent biomarker for evaluating the therapeutic effects of β-blockers.

Acknowledgments

This work was supported by grants-in-aid for scientific research from the Ministry of Education in Japan (Grant Nos. 18591706 to S.K. and 19209030 to M.M.) and the Takeda Science Foundation (2008).

Disclosures

No conflict of interest declared.

References

1. Cohn JN, Levine TB, Olivari MT, Garberg V, Lura D, Francis GS, et al. Plasma norepinephrine as a guide to prognosis in patients with chronic congestive heart failure. *N Engl J Med* 1984; **311:** 819–823.
2. Mann DL, Bristow MR. Mechanisms and models in heart failure: The biomechanical model and beyond. *Circulation* 2005; **111:** 2637–2649.
3. Anand IS, Fisher LD, Chiang YT, Latini R, Masson S, Maggioni AP, et al; Val-HeFT Investigators. Changes in brain natriuretic peptide and norepinephrine over time and mortality and morbidity in the Valsartan Heart Failure Trial (Val-HeFT). *Circulation* 2003; **107:** 1278–1283.
4. Mentz RJ, Felker GM. Natriuretic peptide-guided therapy for heart failure. *Circ J* 2011; **75:** 2031–2037.
5. Maeda K, Tsutamoto T, Wada A, Mabuchi N, Hayashi M, Tsutsui T, et al. High levels of plasma brain natriuretic peptide and interleukin-6 after optimized treatment for heart failure are independent risk factors for morbidity and mortality in patients with congestive heart failure. *J Am Coll Cardiol* 2000; **36:** 1587–1593.
6. Swedberg K, Eneroth P, Kjekshus J, Wilhelmsen L; CONSENSUS Trial Study Group. Hormones regulating cardiovascular function in patients with severe congestive heart failure and their relation to mortality. *Circulation* 1990; **82:** 1730–1736.
7. Tsutamoto T, Wada A, Maeda K, Hisanaga T, Mabuchi N, Hayashi M, et al. Plasma brain natriuretic peptide level as a biochemical marker of morbidity and mortality in patients with asymptomatic or minimally symptomatic left ventricular dysfunction. Comparison with plasma angiotensin II and endothelin-1. *Eur Heart J* 1999; **20:** 1799–1807.
8. Maeda K, Tsutamoto T, Wada A, Hisanaga T, Kinosita M. Plasma brain natriuretic peptide as a biochemical marker of high left ventricular end-diastolic pressure in patients with symptomatic left ventricular dysfunction. *Am Heart J* 1998; **135:** 825–832.
9. Tsutamoto T, Wada A, Maeda K, Hisanaga T, Maeda Y, Fukai D, et al. Attenuation of compensation of endogenous cardiac natriuretic peptide system in chronic heart failure: Prognostic role of plasma brain natriuretic peptide concentration in patients with chronic symptomatic left ventricular dysfunction. *Circulation* 1997; **96:** 509–516.
10. Apple FS, Wu AH, Jaffe AS, Panteghini M, Christenson RH, Cannon CP, et al; National Academy of Clinical Biochemistry; IFCC Committee for Standardization of Markers of Cardiac Damage Laboratory Medicine. National Academy of Clinical Biochemistry and IFCC Committee for Standardization of Markers of Cardiac Damage Laboratory Medicine practice guidelines: Analytical issues for biomarkers of heart failure. *Circulation* 2007; **116:** e95–e98.
11. Braunwald E. Biomarkers in heart failure. *N Engl J Med* 2008; **358:** 2148–2159.
12. Zethelius B, Berglund L, Sundström J, Ingelsson E, Basu S, Larsson A, et al. Use of multiple biomarkers to improve the prediction of death from cardiovascular causes. *N Engl J Med* 2008; **358:** 2107–2116.
13. Iwanaga Y, Miyazaki S. Heart failure, chronic kidney disease, and biomarkers: An integrated viewpoint. *Circ J* 2010; **74:** 1274–1282.
14. Zimmet JM, Hare JM. Nitroso-redox interaction in the cardiovascular system. *Circulation* 2006; **114:** 1531–1544.
15. Bergamini C, Cicoira M, Rossi A, Vassanelli V. Oxidative stress and hyperuricaemia: Pathophysiology, clinical relevance, and therapeutic implications in chronic heart failure. *Eur J Heart Fail* 2009; **11:** 444–452.
16. Banfi C, Brioschi M, Barcella S, Veglia F, Biglioli P, Tremoli E, et al. Oxidized proteins in plasma of patients with heart failure: Role in endothelial damage. *Eur J Heart Fail* 2008; **10:** 244–251.
17. Eleuteri E, Magno F, Gnemmi I, Carbone M, Colombo M, La Rocca G, et al. Role of oxidative and nitrosative stress biomarkers in chronic heart failure. *Front Biosci* 2009; **14:** 2230–2237.
18. Ungvári Z, Gupte SA, Recchia FA, Bátkai S, Pacher P. Role of oxidative-nitrosative stress and downstream pathways in various forms of cardiomyopathy and heart failure. *Curr Vasc Pharmacol* 2005; **3:** 221–229.
19. Tang WHW, Tong W, Troughton RW, Martin MG, Shrestha K, Borowski A, et al. Prognostic value and echocardiographic determinants of plasma myeloperoxidase levels in chronic heart failure. *J Am Coll Cardiol* 2007; **49:** 2364–2370.
20. Wolfram R, Oguogho A, Palumbo B, Sinzinger H. Enhanced oxidative stress in coronary heart disease and chronic heart failure as indicated by an increased 8-epi-PGF(2alpha). *Eur J Heart Fail* 2005; **7:** 167–172.
21. Polidori MC, Praticó D, Savino K, Rokach J, Stahl W, Mecocci P. Increased F2 isoprostane plasma levels in patients with congestive heart failure are correlated with antioxidant status and disease severity. *J Card Fail* 2004; **10:** 334–338.
22. Kameda K, Matsunaga T, Abe N, Hanada H, Ishizaka H, Ono H, et al. Correlation of oxidative stress with activity of matrix metalloproteinase in patients with coronary artery disease. Possible role for left ventricular remodelling. *Eur Heart J* 2003; **24:** 2180–2185.
23. Radovanovic S, Krotin M, Simic DV, Mimic-Oka J, Savic-Radojévic A, Pljesa-Ercegovac M, et al. Markers of oxidative damage in chronic heart failure: Role in disease progression. *Redox Rep* 2008; **13:** 109–116.
24. Kaneko T, Tahara S, Matsuo M. Non-linear accumulation of 8-hydroxy-2'-deoxyguanosine, a marker of oxidized DNA damage, during aging. *Mutat Res* 1996; **316:** 277–285.
25. Ames BN. Endogenous oxidative DNA damage, aging, and cancer. *Free Radic Res Commun* 1989; **7:** 121–128.
26. Loft S, Vistisen K, Ewertz M, Tjonneland A, Overvad K, Poulsen HE. Oxidative DNA damage estimated by 8-hydroxydeoxyguanosine excretion in humans: Influence of smoking, gender and body mass index. *Carcinogenesis* 1992; **13:** 2241–2247.
27. Ide T, Tsutsui H, Hayashidani S, Kang D, Suematsu N, Nakamura K, et al. Mitochondrial DNA damage and dysfunction associated with oxidative stress in failing hearts after myocardial infarction. *Circ Res* 2001; **88:** 529–535.
28. Tsutsui H, Ide T, Shiomi T, Kang D, Hayashidani S, Suematsu N, et al. Oxidative stress mediates tumor necrosis factor-alpha-induced mitochondrial DNA damage and dysfunction in cardiac myocytes. *Circulation* 2001; **104:** 2883–2885.
29. Kono Y, Nakamura K, Kimura H, Nishii N, Watanabe A, Banba K, et al. Elevated levels of oxidative DNA damage in serum and myocardium of patients with heart failure. *Circ J* 2006; **70:** 1001–1005.
30. Kobayashi S, Susa T, Tanaka T, Wada Y, Okuda S, Doi M, et al. Urinary 8-hydroxy-2'-deoxyguanosine reflects symptomatic status and severity of systolic dysfunction in patients with chronic heart failure. *Eur J Heart Fail* 2011; **13:** 29–36.
31. Richardson P, McKenna W, Bristow M, Maisch B, Mautner B, O'Connell J, et al. Report of the 1995 World Health Organization/International Society and Federation of Cardiology Task Force on the Definition and Classification of Cardiomyopathies. *Circulation*

1996; **93:** 841–842.
32. Shikano M, Sobajima H, Yoshikawa H, Toba T, Kushimoto H, Katsumata H, et al. Usefulness of a highly sensitive urinary and serum IL-6 assay in patients with diabetic nephropathy. *Nephron* 2000; **85:** 81–85.
33. Kashiwagi M, Shinozaki M, Hirakata H, Tamaki K, Tadashi H, Tokumoto M, et al. Locally activated rennin-angiotensin system associated with TGF-β1 as a major factor for renal injury induced by chronic inhibition of nitric oxide synthase in rats. *J Am Soc Nephrol* 2003; **11:** 616–624.
34. Mochizuki M, Yano M, Oda T, Tateishi H, Kobayashi S, Yamamoto T, et al. Scavenging free radicals by low-dose carvedilol prevents redox-dependent Ca^{2+} leak via stabilization of ryanodine receptor in heart failure. *J Am Coll Cardiol* 2007; **49:** 1722–1732.
35. Nakamura K, Kusano K, Nakamura Y, Kakishita M, Ohta K, Nagase S, et al. Carvedilol decreases elevated oxidative stress in human failing myocardium. *Circulation* 2002; **105:** 2867–2871.
36. Tsutamoto T, Wada A, Matsumoto T, Maeda K, Mabuchi N, Hayashi M, et al. Relationship between tumor necrosis factor-alpha production and oxidative stress in the failing hearts of patients with dilated cardiomyopathy. *J Am Coll Cardiol* 2001; **37:** 2086–2092.
37. Sawyer DB, Siwik DA, Xiao L, Pimentel DR, Singh K, Colucci WS. Role of oxidative stress in myocardial hypertrophy and failure. *J Mol Cell Cardiol* 2002; **34:** 379–388.
38. Nishiyama K, Tsutamoto T, Yamaji M, Kawahara C, Yamamoto T, Fujii M, et al. Dose-dependent prognostic effect of carvedilol in patients with chronic heart failure: Special reference to transcardiac [corrected] gradient of norepinephrine. *Circ J* 2009; **73:** 2270–2275.
39. Konishi M, Haraguchi G, Kimura S, Inagaki H, Kawabata M, Hachiya H, et al. Comparative effects of carvedilol vs bisoprolol for severe congestive heart failure. *Circ J* 2010; **74:** 1127–1134.

Mitochondrion 12 (2012) 449–458

Contents lists available at SciVerse ScienceDirect

Mitochondrion

journal homepage: www.elsevier.com/locate/mito

Recombinant mitochondrial transcription factor A protein inhibits nuclear factor of activated T cells signaling and attenuates pathological hypertrophy of cardiac myocytes

Takeo Fujino [a], Tomomi Ide [a,*], Masayoshi Yoshida [a], Ken Onitsuka [a], Atsushi Tanaka [a], Yuko Hata [a], Motohiro Nishida [b], Takako Takehara [a], Takaaki Kanemaru [c], Naoyuki Kitajima [b], Shinya Takazaki [d], Hitoshi Kurose [b], Dongchon Kang [d], Kenji Sunagawa [a]

[a] Department of Cardiovascular Medicine, Graduate School of Medical Sciences, Kyushu University, 3-1-1, Maidashi, Higashi-ku, Fukuoka 812-8582, Japan
[b] Department of Pharmacology and Toxicology, Graduate School of Pharmaceutical Sciences, Kyushu University, 3-1-1, Maidashi, Higashi-ku, Fukuoka 812-8582, Japan
[c] Morphology and Core Unit, Kyushu University Hospital, 3-1-1, Maidashi, Higashi-ku, Fukuoka 812-8582, Japan
[d] Department of Clinical Chemistry and Laboratory Medicine, Graduate School of Medical Sciences, Kyushu University, 3-1-1, Maidashi, Higashi-ku, Fukuoka 812-8582, Japan

ARTICLE INFO

Article history:
Received 27 March 2012
Received in revised form 6 June 2012
Accepted 11 June 2012
Available online 16 June 2012

Keywords:
Cardiac hypertrophy
Mitochondrial transcription factor A
Nuclear factor of activated T cells

ABSTRACT

The overexpression of mitochondrial transcription factor A (TFAM) attenuates the decrease in mtDNA copy number after myocardial infarction, ameliorates pathological hypertrophy, and markedly improves survival. However, non-transgenic strategy to increase mtDNA for the treatment of pathological hypertrophy remains unknown. We produced recombinant human TFAM protein (rhTFAM). rhTFAM rapidly entered into mitochondria of cultured cardiac myocytes. rhTFAM increased mtDNA and abolished the activation of nuclear factor of activated T cells (NFAT), which is well known to activate pathological hypertrophy. rhTFAM attenuated subsequent morphological hypertrophy of myocytes as well. rhTFAM would be an attractive molecule in attenuating cardiac pathological hypertrophy.

1. Introduction

Mitochondrial dysfunction has been reported in various forms of heart failure. Mitochondrial DNA (mtDNA) is decreased in the heart from post-myocardial infarction (MI) model in mice (Ide et al., 2001). In human as well, Karamanlidis et al. demonstrated that mitochondrial biogenesis is severely impaired in the myocardium from end-stage heart failure patients. They also showed that there was no significant change in the expression of the fibroblast marker in their sample, suggesting the decrease of mtDNA and mitochondrial biogenesis are not due to the fibrosis occurring under these conditions, changing the ratio of cardiac myocytes with a high amount of mitochondria to fibroblasts and other cell types with low amounts (Karamanlidis et al., 2010). mtDNA could be a major target for locally generated reactive oxygen species (ROS), and an intimate link among mtDNA damage and defects in the electron transport function might play an important role in the development and progression of cardiac remodeling and failure (Ide et al., 2001).

Mitochondrial transcription factor A (TFAM), a nucleus-encoded protein, binding upstream of the light strand and heavy strand promoters of mtDNA, promotes transcription of mtDNA. It also plays an important role in regulating mtDNA copy number (Kanki et al., 2004). TFAM is a high mobility group protein having DNA-binding properties, regardless of its DNA sequence (Parisi and Clayton, 1991). TFAM molecules are abundant enough to cover the entire mtDNA, and indeed most of them bind mtDNA, suggesting that mtDNA is packaged with TFAM (Alam et al., 2003; Kang et al., 2007). Disruption of the *tfam* gene in mice has been shown to cause depletion of mtDNA, loss of mitochondrial transcripts, loss of mtDNA-encoded polypeptides, and severe respiratory chain deficiency (Larsson et al., 1998). Moreover, targeted disruption of *tfam* in cardiac myocytes induced deletion of mtDNA and dilated cardiomyopathy (Li et al., 2000; Wang et al., 1999). In addition, a reduction in TFAM expression has been demonstrated in several forms of cardiac failure (Garnier et al., 2003; Ide et al., 2001; Karamanlidis et al., 2010). We have previously demonstrated in mice, in MI, that TFAM

Abbreviations: mtDNA, mitochondrial DNA; ROS, reactive oxygen species; TFAM, mitochondrial transcription factor A; MI, myocardial infarction; NFAT, nuclear factor of activated T cells; GST, glutathione S-transferase; MTS, mitochondrial targeting signal; rhTFAM, recombinant human TFAM; ΔMTS-rhTFAM, rhTFAM without MTS; rhTFAM-ΔC, rhTFAM lacking C-terminal tail; MAPK, mitogen-activated protein kinase; ERK, extracellular signal-regulated kinase; COX I, cytochrome c oxidase I; COX III, cytochrome c oxidase III; SDHA, succinate dehydrogenase complex subunit A; NDUFA9, NADH dehydrogenase 1 alpha subcomplex subunit 9; ATIII, antithrombin III; RPL27, ribosomal protein L27; MCIP1, modulatory calcineurin interacting protein 1; HPRT, hypoxanthine guanine phosphoribosyl transferase; AngII, angiotensin II; ET-1, endothelin-1; BNP, brain natriuretic peptide.

* Corresponding author. Tel.: +81 92 642 5360; fax: +81 92 642 5374.
E-mail address: tomomi_i@cardiol.med.kyushu-u.ac.jp (T. Ide).

1567-7249/$ – see front matter © 2012 Elsevier B.V. and Mitochondria Research Society. All rights reserved.
doi:10.1016/j.mito.2012.06.002

overexpression attenuated the decrease in mtDNA copy number, ameliorated pathological hypertrophy, and dramatically improved survival rate (Ikeuchi et al., 2005). In addition, the overexpression of TFAM in Hela cells reduced mitochondrial ROS generation (Hayashi et al., 2008). Taken together, these findings indicate that upregulating TFAM results in increasing mtDNA copy number and attenuates cardiac pathological hypertrophy. However, the effective way how to increase TFAM expression or mtDNA copy number in clinical situation remains unknown.

Recent study showed that exogenously administered recombinant TFAM engineered with an N-terminal protein transduction domain, followed by a matrix mitochondrial localization sequence, was recruited into mitochondria of cultured cells (Iyer et al., 2009). Therefore it is conceivable that exogenously administered recombinant TFAM manifests beneficial impacts on myocytes, and this method could be useful for the therapy of cardiac pathological hypertrophy. In the present study, we examined whether exogenous recombinant TFAM protein was recruited into cardiac myocytes and functioned to increase mtDNA copy number and attenuate hypertrophy of myocytes in vitro. The results indicated that recombinant TFAM protein inhibited nuclear factor of activated T cells (NFAT) signaling and prevented pathological hypertrophy of cardiac myocytes.

2. Material and methods

2.1. Preparation of human TFAM protein

We used a glutathione S-transferase (GST) gene fusion purification protocol to synthesize recombinant human TFAM protein. Two TFAM proteins, rhTFAM (recombinant human TFAM with mitochondrial targeting signal (MTS)) and ΔMTS-rhTFAM (recombinant human TFAM without MTS), were prepared. The nucleotide sequences corresponding to human TFAM and TFAM without MTS were cloned from human cDNA library, and were subcloned into pGEX-6P-1 (GE Healthcare). The constructs were transformed into competent cells (BL21 (DE3), Invitrogen). The transformed bacteria were cultured in LB medium (MP Biochemicals) supplemented with 100 μg/ml ampicillin (Wako), in the shaking incubator (Bio-Shaker BR-300LF, TAITEC). When the culture achieved an optical density of wavelength 600 nm to 0.5–0.7, isopropyl-β-D-thiogalactopyranoside (0.7 mM, nacalai tesque) was added to the medium and incubated for further 2 h. Growth and expression of the bacteria culture were performed at 37 °C with variable agitation and airflow. The bacteria were harvested and pelleted by centrifugation at 8000g and stored at −80 °C.

Cell pellets were resuspended in sonication buffer (20 mM Tris–HCl, 500 mM NaCl, 250 mM, 2-mercaptoethanol 5 mM, 1% NP-40 and protease inhibitor cocktail (Complete Mini, Roche Diagnostics)) and mildly sonicated at 4 °C. The lysate was then clarified by centrifugation at 8000g for 30 min. The supernatant was mixed with Glutathione Sepharose 4B resin (GE Healthcare) for 2 h and applied to polypropylene columns (Thermo SCIENTIFIC). Resin absorbed with GST-TFAM protein was washed with wash buffer (20 mM Tris–HCl, 150 mM NaCl, 5 mM 2-mercaptoethanol, 0.1% NP-40) to isolate the vector protein. Then it was mixed with Turbo3C Protease (160 units/ml, Accelagen) and elusion buffer (20 mM Tris–HCl, 150 mM NaCl, 5 M 2-mercaptoethanol, 0.1% NP-40) at 4 °C overnight to remove GST from TFAM. The flow-through was collected and dialyzed with Slide-a-lyzer Dialysis Cassette (7 K MWCO, Thermo Scientific) in phosphate buffered saline (PBS). The solution was screened via sodium dodecyl sulfate (SDS)–polyacrylamide gel electrophoresis (PAGE) analysis for proper size and purity. The purity was above 98% by Coomassie Brilliant Blue (CBB) staining. Western blot analysis was also performed using anti-human TFAM specific antibody to verify the success of target protein purification (Fig. 1). The solution was stored at −80 °C and used as recombinant TFAM protein. We also performed the same procedure using empty vector without TFAM sequence and the product was also stored at −80 °C. In addition, we synthesized recombinant human TFAM lacking the C-terminal 25

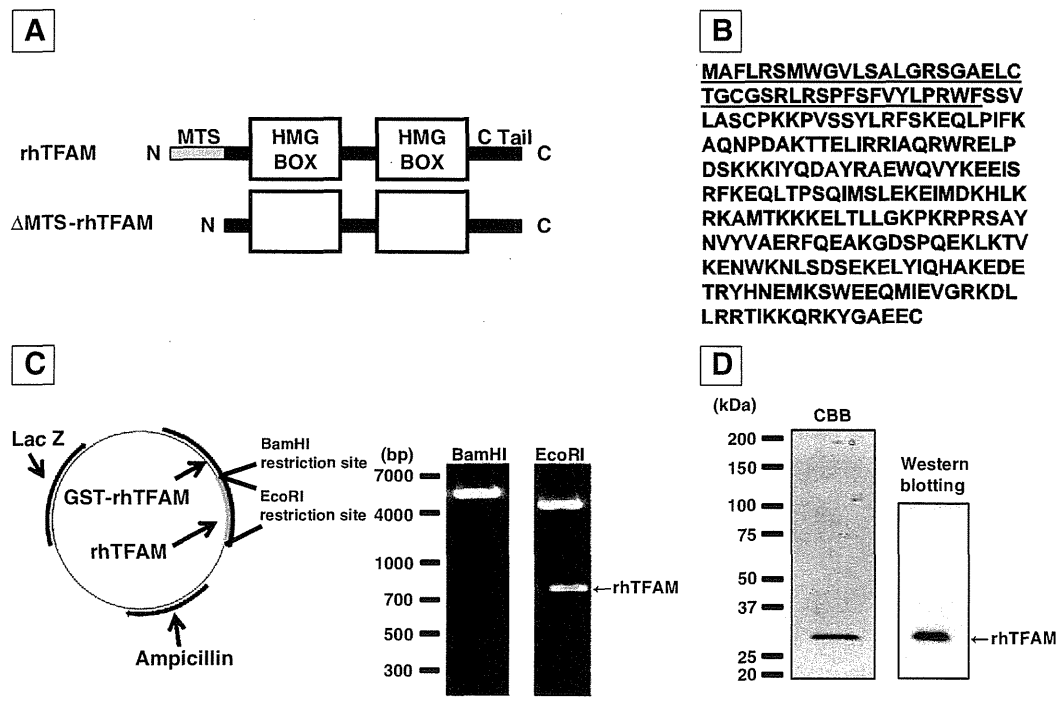

Fig. 1. Synthesis of recombinant human TFAM protein. (A and B) Schematic structure (A) and amino acid sequence (B) of human TFAM protein. Underlined part is MTS. (C) Schematic structure and electrophoresis of pGEX-6P-1-TFAM, the subcloned plasmid we constructed for synthesizing recombinant TFAM. TFAM sequence was inserted between the EcoRI restriction sites. The left lane shows linear whole plasmid (BamHI restriction), and the right lane shows electrophoretically separated pGEX-6P-1 and TFAM (EcoRI restriction). (D) SDS-PAGE analysis of the product. We confirmed the product as TFAM by CBB staining (left lane) and Western blotting using human TFAM -specific antibody (right lane).

amino acids (rhTFAM-ΔC) as described previously (Ohgaki et al., 2007).

2.2. Preparation and culture of cardiac myocytes and RAW 264.7 cells

All procedures and animal care were approved by the Committee on Ethics of Animal Experiment, Kyushu University Graduate School of Medical and Pharmaceutical Sciences and performed in accordance with the Guideline for Animal Experiment of Kyushu University, and the Guide for the Care and Use of Laboratory Animals published by the US National Institutes of Health (NIH Publication No. 85–23, revised 1996). Primary culture of neonatal rat ventricular myocytes was prepared from the ventricles of neonatal SD rats as described previously (Tsutsumi et al., 2008). Neonatal rats were euthanized by decapitation under anaesthesia with isoflurane, after which the hearts were rapidly excised and digested. Anaesthesia depth was monitored by limb withdrawal using toe pinching. After digestion of the myocardial tissue with trypsin (Wako) and collagenase type 2 (Worthington), cells were suspended in Dulbecco's Modified Eagle's Medium (Sigma-Aldrich) containing 10% fetal bovine serum (FBS, Thermo Scientific), penicillin (Invitrogen) and streptomycin (Invitrogen), and plated twice in 100 mm culture dishes (Cellstar, greiner bio-one) for 70 min each to reduce the number of non-myocytes. Non-adherent cells were plated in culture dishes (Primaria, Falcon) at an appropriate density for each experiment. Myocytes were maintained at 37 °C in humidified air with 5% CO_2 for 36 h after the plating to the culture dishes. The culture medium was changed and rhTFAM protein was added to the medium 12 h before each experiment.

RAW 264.7 cells, mouse leukemic monocyte macrophage cell line, were originally obtained from American Type Culture Collection (ATCC; cat.no.TIB-71).

2.3. Western blot analyses

Western blot analysis of cardiac myocytes was performed as described previously (Kanki et al., 2004). Cells were carefully washed with Hanks' balanced salt solution (HBSS, Invitrogen) and collected in lysis buffer (RIPA Buffer, Thermo Scientific) with protease inhibitor cocktail. Equal amounts of protein (10 μg protein per lane), estimated by the bicinchoninic acid assay with the use of BCA Protein Assay (Thermo Scientific), were separated on SDS-PAGE and then electrophoretically transferred to a nitrocellulose membrane (Trans-Blot, Bio-Rad). After blocking for 2 h, the membrane was incubated with a certain primary antibody at 4 °C overnight. Then they were incubated with corresponding secondary antibody for 1 h at room temperature. The chemiluminescence was detected with an ECL™ Western Blotting Detection Reagents (GE Healthcare) according to the manufacturer's recommendation. The signal was visualized and recorded with a chilled charge-coupled device camera, LAS3000 (FUJIFILM). We also performed the same procedure using RAW 264.7 cells.

Antibody to human TFAM was produced by immunizing rabbits with recombinant human TFAM. Antibodies to cytochrome c oxidase I (COX I), cytochrome c oxidase III (COX III), succinate dehydrogenase complex subunit A (SDHA), and NADH dehydrogenase 1 alpha subcomplex subunit 9 (NDUFA9) were from Invitrogen. Antibody to glyceraldehyde 3-phosphate dehydrogenase (GAPDH) and secondary antibodies for Western blotting were obtained from Santa Cruz Biotechnology. Densities of the immunoreactive bands were evaluated using NIH ImageJ software, and relative amounts were quantified relative to GAPDH.

For the measurement of mitogen-activated protein kinase (MAPK) p44/42 (extracellular signal-regulated kinase (ERK) 1/2)) phosphorylation, cells were stimulated with endothelin-1 (ET-1, 100 nM, Sigma-Aldrich) for 30 min and collected. Antibodies to phospho-MAPK p44/42 and total-MAPK p44/42 were from Invitrogen. Total-MAPK p44/42 protein contents were also determined after stripping the phosphoblots with stripping solution (nacalai tesque) in order to verify for protein loading. Signal intensities were quantified as the ratio of phospho- to total-MAPK p44/42.

2.4. Immunostaining

Cells were washed with HBSS and treated with 500 nM MitoTracker Orange (Invitrogen) in culture medium for 15 min. They were again washed with HBSS and fixed with −20 °C methanol for 20 min. After blocking with the mixture of 10% FBS and 1% bovine serum albumin (Wako), they were incubated with anti-human TFAM antibody at 4 °C overnight. Then they were incubated with fluorescence-labeled secondary antibody (Alexa Fluor 488 chicken anti-rabbit IgG, Invitrogen) for 1 h. They were mounted with mounting medium with DAPI (Vectashield, Vector Laboratories) and observed by confocal microscopy (A1, Nikon).

2.5. Cell viability

Cell viability was measured using Cell Counting Kit-8 (Dojindo) as manufacturer's protocol. Briefly, the reagent was added to the culture medium and incubated for 3 h. Then the absorbance of the culture medium at 450 nm was measured by the microplate reader (Infinite 200, TECAN).

2.6. Lactate dehydrogenase (LDH) Assay

LDH concentration in the culture medium was measured using LDH-Cytotoxicity Assay Kit (Wako) as manufacturer's protocol. Briefly, the culture medium was reacted with the reagent for 30 min at room temperature. Then the absorbance at 560 nm was measured by the microplate reader.

2.7. Observation by transmission electron microscopy (TEM)

Cardiac myocytes were collected and fixed with 2% glutaraldehyde (TAAB), post-fixed in 1% osmium tetroxide, and embedded. Ultrathin sections were post-stained with Sato's lead staining solution and observed with TEM (H7000E, Hitachi).

2.8. Real-time polymerase chain reaction (PCR) analyses

mtDNA copy number and mRNA expression were quantified by real-time PCR analysis, as described previously (Kanki et al., 2004; Lagouge et al., 2006). Total DNA was extracted with DNeasy tissue kit (Qiagen), and total RNA was extracted with RNeasy tissue kit (Qiagen). The total DNA or RNA was quantified by absorbance method (BioPhotometer, Eppendorf).

Total DNA was treated with BamHI (Takara) for 6 h and the relative amount of mtDNA was quantified by quantitative PCR. The PCR mixture contained 3 ng of the total DNA, 12 pmol each of primers (5′-ACTCCCTATTCGGAGCCCTA-3′ and 5′-GGAGCTCGATTTGTTTCTGC-3′ for mtDNA) in 30 μl. To estimate the amount of genomic DNA as an internal standard, antithrombin III (ATIII) gene was amplified in a 30 μl reaction mixture containing 3 ng of the total DNA, 12 pmol each of primers (5′-TGCTACTCATTGGTGCCTTG-3′ and 5′-TTCCGGAACCTTCTGCTCTA-3′). The amount of mtDNA was adjusted to the amount of genomic DNA. All reactions were performed with SYBR Premix Ex Taq II (Takara) and Applied Biosystems 7500 Real-Time PCR system (Applied Biosystems) according to the manufacture's protocol. We also confirmed the result using another primer set for mtDNA (5′-CCCAGCCACCACTATCATTC-3′ and 5′-TGATGTTGGGGTTATGTTGG-3′). We also performed the same procedure using RAW 264.7 cells, using the primer set for mtDNA (5′-TGTAAGCCGGACTGCTAATG-3′ and 3′-AGCTGGAGCCGTAATTACAG-5′)